

# Nitrido Dimers and Trimers of Tungsten Supported by *t*BuMe<sub>2</sub>SiO and CF<sub>3</sub>Me<sub>2</sub>CO Ligands, Respectively. Factors Influencing the Reductive Cleavage of Nitriles by Tungsten–Tungsten Triple Bonds and An Analysis of the Structure of the Cyclotrimer

Malcolm H. Chisholm,<sup>\*[a]</sup> Kirsten Folting,<sup>[a]</sup> Matthew L. Lynn,<sup>[a]</sup> Darin B. Tiedtke,<sup>[a]</sup> Frédéric Lemoigno,<sup>[b]</sup> and Odile Eisenstein<sup>\*[b]</sup>

Dedicated to Professor Roald Hoffmann on entering his seventh decade

**Abstract:** [W<sub>2</sub>(OR)<sub>6</sub>] compounds (R = *t*BuMe<sub>2</sub>Si and CF<sub>3</sub>Me<sub>2</sub>C) are shown to react reversibly with nitriles (MeCN and ArCN) in [D<sub>8</sub>]toluene to give [W<sub>2</sub>(OR)<sub>6</sub>L<sub>2</sub>] compounds (L = nitrile). For MeCN the enthalpy of adduct formation for [M<sub>2</sub>(OCCF<sub>3</sub>Me<sub>2</sub>)<sub>6</sub>] favors tungsten over molybdenum:  $\Delta H^\circ = 22(1) \text{ kcal mol}^{-1}$  (M = Mo) vs.  $\Delta H^\circ = -26(1) \text{ kcal mol}^{-1}$  (M = W), while for both metals the  $\Delta S^\circ$  values were about  $-80 \text{ eu}$ . From an <sup>15</sup>N NMR line-shape analysis the activation parameters for adduct formation are calculated to be  $\Delta H^\ddagger = +24(2) \text{ kcal mol}^{-1}$  and  $\Delta S^\ddagger = 36(6) \text{ eu}$  for M = W and  $\Delta H^\ddagger = 19(2) \text{ kcal mol}^{-1}$  and  $\Delta S^\ddagger = -38(6) \text{ eu}$  for M = Mo. Adduct formation is less favored for benzonitrile with  $\Delta H^\circ = -16(1) \text{ kcal mol}^{-1}$  for the formation of [W<sub>2</sub>(OCMe<sub>2</sub>CF<sub>2</sub>)<sub>6</sub>(NCC<sub>6</sub>H<sub>5</sub>)<sub>2</sub>]. However, the reductive cleavage of PhC≡N is favored kinetically over MeC≡N and

only occurs for M = W. For reactions between [W<sub>2</sub>(OCCF<sub>3</sub>Me<sub>2</sub>)<sub>6</sub>] and PhCN (10, 20 and 30 equivalents of PhCN) the rate is retarded with increasing nitrile concentration. The activated species is proposed to be a monoadduct [W<sub>2</sub>(OR)<sub>6</sub>(μ-NCPH)]. The products of the cleavage are [NW(OR)<sub>3</sub>]<sub>n</sub> and MeC≡CMe or ArC≡CAr for MeC≡N and PhC≡N, respectively, as determined by <sup>13</sup>C and <sup>15</sup>N labeling studies. For R = *t*BuMe<sub>2</sub>Si a dimeric structure is obtained with terminal nitride ligands and bridging OS*t*BuMe<sub>2</sub> ligands. For R = CCF<sub>3</sub>Me<sub>2</sub>, a cyclotrimer exists both in solution and the solid state, with a planar W<sub>3</sub>N<sub>3</sub> ring with alternating short and

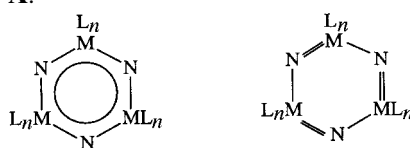
long W–N distances. The structure of the model compound [(HO)<sub>3</sub>WN]<sub>3</sub> has been investigated by DFT (B3LYP) calculations. The short–long alternating WN bond lengths of the ring are well reproduced and are attributed to the preference for the OR groups to occupy two equatorial and one axial site of the trigonal bipyramid at each W center. Models of transition states were studied and support the absence of site exchange at each tungsten; this would have led to an interchange of the short and long W–N bonds. These findings are discussed in terms of the earlier predictions of Hoffmann et al. and the experimental findings of other workers for d<sup>0</sup> metal nitrides of formula [L<sub>n</sub>MN]<sub>3</sub>. The cell parameters for [(CF<sub>3</sub>Me<sub>2</sub>CO)<sub>3</sub>WN]<sub>3</sub> at  $-169^\circ\text{C}$  are:  $a = 22.481(5)$ ,  $b = 11.367(2)$ ,  $c = 22.573(2) \text{ \AA}$ ,  $\beta = 94.6(1)^\circ$  and space group  $P2_1/c$ .

**Keywords:** alkoxides • density functional calculations • molecular orbitals • nitrides • nitrile cleavage • tungsten

## Introduction

As in so many areas of organometallic and coordination chemistry, it was Roald Hoffmann<sup>[1]</sup> who first applied the

broad stroke of his pen to describe the bonding modes in transition metal nitrides complexes. In a paper entitled “Transition Metal Nitrides, Organic Polyenes and Phosphazenes. A Structural and Orbital Analogy” the authors stated, “Perhaps the most interesting conclusion we can draw for transition metal nitrides is that there should be substantial stability for a benzene analogue. Does this mean that the benzene analogue will have all equal bond lengths, we are not sure.” Hoffmann et al. drew the limiting structures shown in **A**.<sup>[1]</sup>



**A**

[a] Prof. M. H. Chisholm, K. Folting, M. L. Lynn, Dr. D. B. Tiedtke  
Department of Chemistry and Molecular Structure Center  
Indiana University, Bloomington, IN 47405 (USA)  
Fax: (1)812855-7148  
E-mail: chisholm@indiana.edu

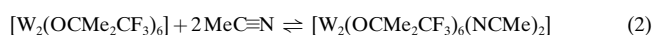
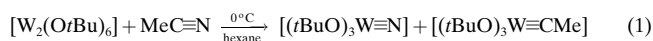
[b] Prof. O. Eisenstein, F. Lemoigno  
Laboratoire de Structure et Dynamique  
des Systèmes Moléculaires et Solides, Case Courrier 14  
(UMR 5636) Université de Montpellier 2  
F-34095 Montpellier Cedex 5 (France)

Shortly thereafter Roesky<sup>[2]</sup> and then Wolczanski<sup>[3]</sup> reported the structure of the cyclotrimers  $[\text{Cp}^*\text{Ta}(\text{X})\text{N}]_3$ , where X = Cl and Me, which contained a planar  $\text{M}_3\text{N}_3$  moiety with statistically equivalent Ta–N bond lengths (1.84(2) to 1.90(2) Å). Wolczanski et al.<sup>[3]</sup> carried out extended Hückel calculations on an idealized  $[\text{X}_2\text{TaN}]_3$  molecule with  $\text{C}_{3v}$  symmetry and established that the trimer had the familiar  $\pi$ -type MO's with a and e symmetry as in benzene.

In this paper we describe our continuing studies of substrate uptake and activation at dimolybdenum and ditungsten centers supported by alkoxide ligands,<sup>[4]</sup> which by cleavage of the C–N triple bond of organic nitriles have led to the isolation of  $[(\text{RO})_3\text{WN}]_n$  compounds. When  $\text{R} = t\text{BuMe}_2\text{Si}$ , the complex is a dimer,  $n = 2$ , with terminal nitrido ligands, and when  $\text{R} = \text{CF}_3\text{Me}_2\text{C}$  the complex is a cyclotrimer,  $n = 3$ , with alternating short and long W–N bond lengths. A preliminary account of this work has been published.<sup>[5]</sup>

## Results and Discussion

**Syntheses and reactivity studies:** The reactivity of a metal–metal triple bond is greatly influenced by the metal, the M–M electronic configuration, and the set of attendant ligands. For  $[\text{M}_2(\text{OtBu})_6]$  compounds the importance of the metal, M = Mo versus W, is seen in the fact that  $[\text{Mo}_2(\text{OtBu})_6]$  fails to react with  $\text{MeC}\equiv\text{N}$ , whereas  $[\text{W}_2(\text{OtBu})_6]$  shows an extremely rapid reaction to give products of the reductive cleavage of the C–N triple bond [Eq. (1)].<sup>[7]</sup> Upon changing the ligands from  $t\text{BuO}$  to  $\text{CF}_3\text{Me}_2\text{CO}$  Schrock and co-workers noted that  $[\text{W}_2(\text{OCMe}_2\text{CF}_3)_6]$  reacts reversibly with acetonitrile to form a bis-nitrile adduct [Eq. (2)].<sup>[8]</sup>



We have confirmed this observation and, by use of  $^{15}\text{N}$  NMR spectroscopy and the labeled acetonitrile  $\text{MeC}\equiv^{15}\text{N}$ , we have measured the equilibrium constants at various temperatures in  $[\text{D}_8]\text{toluene}$ . A similar equilibrium was established for  $[\text{Mo}_2(\text{OCMe}_2\text{CF}_3)_6]$  and this has allowed us to compare the thermodynamic parameters, which are  $\Delta H^\circ = -22(1) \text{ kcal mol}^{-1}$  for  $\text{M} = \text{Mo}$  and  $26(1) \text{ kcal mol}^{-1}$  for  $\text{M} = \text{W}$ . This is consistent with our earlier measurements of the relative binding of Lewis bases to related  $[\text{M}_2(\text{OR})_6]$  compounds; this revealed that tungsten binds ligands more strongly, but only by about  $3 \text{ kcal mol}^{-1}$ .<sup>[4]</sup> It is also consistent with the generally held opinion and truism that metal–ligand bonds to third row transition metal elements are stronger than related bonds involving second row elements because of the greater radial extension of the 5d relative to the 4d atomic orbitals. This same effect is seen in metal–metal bond strengths and the heats of sublimation of the elements,  $\Delta H_{\text{subm}} \text{ W} > \text{Mo}$ .<sup>[9]</sup> The entropies of formation,  $\Delta S^\circ$ , of the bis-acetonitrile adducts,  $[\text{M}_2(\text{OCMe}_2\text{CF}_3)_6(\text{NCMe})_2]$  were  $-84(4) \text{ eu}$  ( $\text{M} = \text{W}$ ) and  $-78(4) \text{ eu}$  ( $\text{M} = \text{Mo}$ ). These values are large as might be expected for a reaction wherein three molecules are involved in adduct formation:  $\text{A} + 2\text{B} \rightarrow \text{C}$ . They are statistically the same for  $\text{M} = \text{Mo}$  and  $\text{W}$  and the  $\Delta S^\circ$

value is roughly twice that seen in the formation of mono adducts of  $[\text{M}_2(\text{OR})_6]$  compounds, such as in the reaction between  $[\text{Mo}_2(\text{OCH}_2t\text{Bu})_6]$  and both  $\text{P}(n\text{Bu})_3$  and  $\text{NCNEt}_2$ .<sup>[4]</sup>

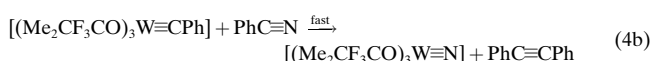
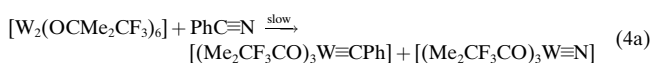
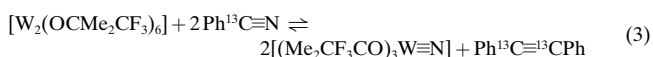
The equilibrium in Equation (2), which was followed as a function of temperature by  $^{15}\text{N}$  NMR spectroscopy, also allowed an estimation of the activation parameters from a simulation of the line broadening of the bound and free  $\text{MeC}^{15}\text{N}$  signals. For  $\text{M} = \text{W}$ , we estimate  $\Delta H^\ddagger = 24(2) \text{ kcal mol}^{-1}$  and  $\Delta S^\ddagger = -38(6) \text{ eu}$ , and from studies of the related reaction involving  $[\text{Mo}_2(\text{OCMe}_2\text{CF}_3)_6]$  and  $\text{MeC}^{15}\text{N}$   $\Delta H^\ddagger = 19(2) \text{ kcal mol}^{-1}$  and  $\Delta S^\ddagger = -38(6) \text{ eu}$  for  $\text{M} = \text{Mo}$ .

These data provide a consistent picture for the reaction wherein the trends in the enthalpy of activation and entropy of activation differ little for the two metals (molybdenum appearing slightly more labile) and only half of the overall entropy loss is seen in the  $\Delta S^\ddagger$  values.

Although the reversibility of the reaction in Equation (2) reported by Schrock<sup>[8]</sup> was readily confirmed, we did observe that at room temperature there was a slow further reaction to give  $[(\text{Me}_2\text{CF}_3\text{CO})_3\text{W}\equiv\text{N}]_3$ . This occurred over a period of two weeks in the presence of an approximate 10-fold excess of  $\text{MeCN}$  at room temperature. The reaction was most clean when  $\text{MeC}\equiv\text{CMe}$ , which was also formed in this reaction, was allowed to escape from the reaction mixture, because otherwise  $\text{MeC}\equiv\text{CMe}$  and  $[\text{W}_2(\text{OCMe}_2\text{CF}_3)_6]$  react.<sup>[8]</sup> No similar cleavage of  $\text{MeC}\equiv\text{N}$  was observed for  $[\text{Mo}_2(\text{OCMe}_2\text{CF}_3)_6]$  over a period of months.

The reaction between benzonitrile and  $[\text{W}_2(\text{OCMe}_2\text{CF}_3)_6]$  in  $[\text{D}_8]\text{toluene}$  was also studied. This too showed an equilibrium of the type shown in Equation (2) and, by use of  $^{13}\text{C}$  NMR spectroscopy and reactions employing  $\text{Ph}^{13}\text{C}\equiv\text{N}$ , we determined  $\Delta H^\circ = -16(1) \text{ kcal mol}^{-1}$  and  $\Delta S^\circ = -38(4) \text{ eu}$ . The smaller enthalpy of formation of  $[\text{W}_2(\text{OCMe}_2\text{CF}_3)_6(\text{NCPh})_2]$ ,  $\Delta H^\circ = -16(1) \text{ kcal mol}^{-1}$  relative to the acetonitrile adduct,  $\Delta H^\circ = -26(1) \text{ kcal mol}^{-1}$ , is understandable in that  $\text{MeCN}$  is a better (stronger) Lewis base than benzonitrile. However, the markedly lower value of  $\Delta S^\circ = -38(4) \text{ eu}$  for  $\text{PhCN}$  relative to  $-78(4) \text{ eu}$  for  $\text{MeCN}$  is harder to explain. It does mean, however, that while enthalpically the acetonitrile adduct is favored, and this is seen in the position of equilibrium at room temperature, with increasing temperature the  $-T\Delta S^\circ$  term will increase significantly and more rapidly for  $\text{MeCN}$  thus favoring dissociation at higher temperatures.

Studies of the binding of  $\text{Ph}^{13}\text{CN}$  were complicated by the reaction shown in Equation (3), which proceeds at a significant rate at  $30^\circ\text{C}$ . The formation of  $\text{Ph}^{13}\text{C}\equiv^{13}\text{CPh}$  is readily followed by  $^{13}\text{C}$  NMR spectroscopy as is the loss of  $\text{Ph}^{13}\text{C}\equiv\text{N}$ . It is a very clean reaction and almost certainly proceeds by the two step reaction sequence shown in Equations (4a) and (4b).

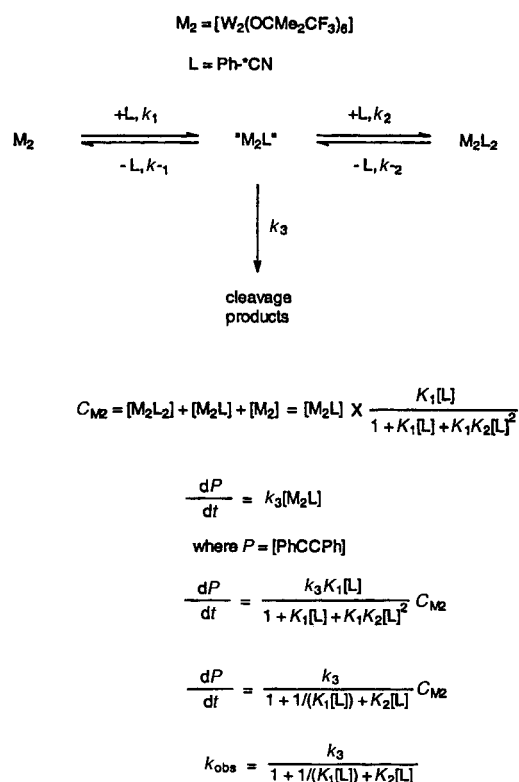


We have found no evidence for the intermediacy of the benzyldiyne complex  $[(\text{Me}_2\text{CF}_3\text{CO})_3\text{W}\equiv^{13}\text{CPh}]$  by  $^{13}\text{C}\{^1\text{H}\}$ NMR spectroscopy; this implies that the reaction in Equation (4b) is notably faster than that in Equation (4a). Even in the presence of only one equivalent of  $\text{Ph}^{13}\text{C}\equiv\text{N}$ , we observed formation of  $[(\text{Me}_2\text{CF}_3\text{CO})_3\text{W}\equiv\text{N}]$  and  $\text{Ph}^{13}\text{C}\equiv^{13}\text{CPh}$  along with unreacted  $[\text{W}_2(\text{OCMe}_2\text{CF}_3)_6]$ . There is good precedent for the metathesis reaction between a nitrile and a terminal alkylidyne leading to  $\text{M}\equiv\text{N}$  and  $\text{C}\equiv\text{C}$  functionalities.<sup>[10]</sup>

At this point it is worth mentioning the following observations. 1)  $\text{PhCN}$  and  $[\text{Mo}_2(\text{OCMe}_2\text{CF}_3)_6]$  enter into a reversible equilibrium with the formation of  $[\text{Mo}_2(\text{OCMe}_2\text{CF}_3)_6(\text{NCPh})_2]$ , but even after several weeks we found no evidence for a further reaction analogous to that in Equation (3). 2) Under the conditions of 10 equivalents of nitrile to 1 equivalent of  $[\text{W}_2(\text{OCMe}_2\text{CF}_3)_6]$ , we observed that there was a significant difference in the rates of the reactions of  $p\text{-XC}_6\text{H}_4\text{CN}$  compounds toward  $\text{C}\equiv\text{N}$  bond cleavage, such that the observed rates were in the order  $\text{CF}_3 > \text{Cl} > \text{H} > \text{OMe}$ . In no instance was cleavage observed in reactions with  $[\text{Mo}_2(\text{OCMe}_2\text{CF}_3)_6]$ , though reversible adduct formation akin to that in Equation (2) was seen.

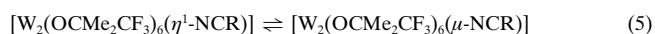
The reaction between  $\text{Ph}^{13}\text{C}\equiv\text{N}$  and  $[\text{W}_2(\text{OCMe}_2\text{CF}_3)_6]$  was studied as a function of temperature for reactions involving 10 equivalents of  $\text{Ph}^{13}\text{C}\equiv\text{N}$  to 1 equivalent of  $[\text{W}_2(\text{OCMe}_2\text{CF}_3)_6]$  and at  $48.6^\circ\text{C}$  with varying initial concentrations of  $[\text{Ph}^{13}\text{CN}]$  to  $[\text{W}_2(\text{OCMe}_2\text{CF}_3)_6]$  ranging from 10:1 to 2:1. Based on these studies we propose the reaction pathway shown in Scheme 1.

The essential feature of Scheme 1 is that the reversible equilibrium [Eq. (2)] proceeds in a stepwise manner involving

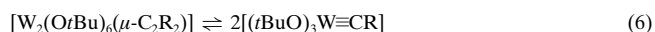


Scheme 1.

a monoadduct  $[\text{W}_2(\text{OCMe}_2\text{CF}_3)_6(\text{NCR})]$  that exists in dynamic exchange with  $[\text{W}_2(\text{OCMe}_2\text{CF}_3)_6]$ , free  $\text{RCN}$ , and  $[\text{W}_2(\text{OCMe}_2\text{CF}_3)_6(\text{NCR})_2]$ . It is, however, from the monoadduct that the products of the reductive cleavage are formed and it is possible to introduce yet another equilibrium step [Eq. (5)] involving an  $\eta^1\text{-NCR}$  complex and a  $\mu\text{-NCR}$  species.



The nature of the  $\mu\text{-NCR}$  complex is unknown and could have the form of a parallel bridged species as seen in the structure of  $[\text{Mo}_2(\text{OCH}_2t\text{Bu})_6(\mu\text{-NCNMe}_2)]^{[11]}$  or a perpendicular bridge as seen by Eglin<sup>[12]</sup> and Cotton<sup>[13]</sup> in which a  $\mu\text{-NCMe}$  ligand bridges a  $\text{Mo}_2^{4+}$  or  $\text{W}_2^{4+}$  center. We have tried to find NMR evidence for a monoadduct  $[\text{W}_2(\text{OCMe}_2\text{CF}_3)_6(\text{NCR})]$ , where  $\text{R} = \text{Me}$  and  $\text{Ph}$ , by studies employing the  $^{15}\text{N}$  or  $^{13}\text{C}$  labeled nitriles in which the concentration of nitrile to  $\text{W}_2$  complex was less than 1:1, but only free nitrile, the  $\text{W}_2$  complex, and the bis-nitrile adduct were detected by NMR spectroscopy. Never-the-less it is almost certain that the products of the reductive cleavage of the nitrile are derived from the monobridged adduct just as in the cleavage of alkynes for which we have established, in certain cases, the reversible equilibrium [Eq. (6)], involving the  $\mu\text{-alkyne}$  adduct.<sup>[14]</sup>



From the proposed reaction sequence presented in Scheme 1 we can determine that  $k_{\text{obs}}$  is the complex expression shown in Equation (7), where  $K_1$  and  $K_2$  refer to the equilibrium constants for the formation of the mono- and bis-nitrile adducts, respectively.

$$k_{\text{obs}} = \frac{k_3}{1 + 1/(K_1[\text{L}] + K_2[\text{L}])} \quad (7)$$

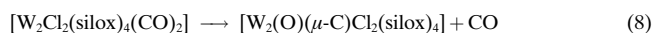
The pseudo-first-order rate constants for the cleavage of benzonitrile at  $48.6^\circ\text{C}$  as a function of benzonitrile concentration are given in Table 1. Here it is evident that the rate of

Table 1. Pseudo-first-order rate constant for cleavage of benzonitrile by  $[\text{W}_2(\text{OCMe}_2\text{CF}_3)_6]$ .

Initial $[\text{Ph}^*\text{CN}]/[\text{W}_2]$ ratio	$[\text{Ph}^*\text{CN}]$ [M]	$k_{\text{obs}}$ [ $\times 10^5 \text{ s}^{-1}$ ]
10	0.1686	2.79
5	0.08430	7.24
3	0.05056	17.2
2	0.03372	32.6

cleavage is suppressed by benzonitrile, but a simple inverse relationship  $k_{\text{obs}} \sim 1/[\text{PhC}\equiv\text{N}]$  was not observed. In this respect it is interesting to note the similarity and difference between the present study and that of Wolczanski et al.<sup>[15]</sup> who studied the cleavage of carbon monoxide at a  $(\text{W}\equiv\text{W})^{6+}$  center in the reaction shown in Equation (8). In Equation (8) the reaction proceeds only at elevated temperatures and shows a strict inverse dependence on the concentration of added CO (silox =  $\text{OSi}t\text{Bu}_3$ ). Here the dicarbonyl adduct is strongly

avored on enthalpic grounds. The  $K_1$  value is very large and, thus, the term  $1/(K_1[L])$  approaches zero, such that the term  $K_2[L]$  in the denominator is rate limiting.



The influence of temperature on the rate of the reaction is revealed by the data presented in Table 2. As one would expect, the rate increases with temperature. The reaction was

Table 2.  $k_{\text{obs}}$  for benzonitrile cleavage reactions.

$T$ [°C]	[Ph- $^{13}\text{C}\equiv\text{N}$ ]	$k_{\text{obs}}$ [s $^{-1}$ ]
34.7	0.1718	$5.20 \times 10^{-6}$
39.7	0.1707	$9.95 \times 10^{-6}$
43.5	0.1697	$1.53 \times 10^{-5}$
48.6	0.1686	$2.83 \times 10^{-5}$
55.2	0.1675	$3.70 \times 10^{-5}$
60.1	0.1664	$5.17 \times 10^{-5}$
64.9	0.1653	$6.29 \times 10^{-5}$

monitored with 10 equivalents of PhCN and the *initial rate of reaction* was estimated and taken as  $k_{\text{obs}}$ . It is important to recognize here that the formation of  $[(\text{Me}_2\text{CF}_3\text{CO})_3\text{W}\equiv\text{N}]$  and PhC $\equiv$ CPh consumes 2 equivalents of PhC $\equiv$ N per one equivalent of  $[\text{W}_2(\text{OCMe}_2\text{CF}_3)_6]$ , and, since the rate of the reaction changes with concentration of [PhC $\equiv$ N] in a non-linear manner,  $k_{\text{obs}}$  is not constant over the course of the reaction. A plot of  $\ln(k_{\text{obs}}/T)$  versus  $1/T$  is shown in Figure 1. The nonlinear plot shows that the rate data do not conform to

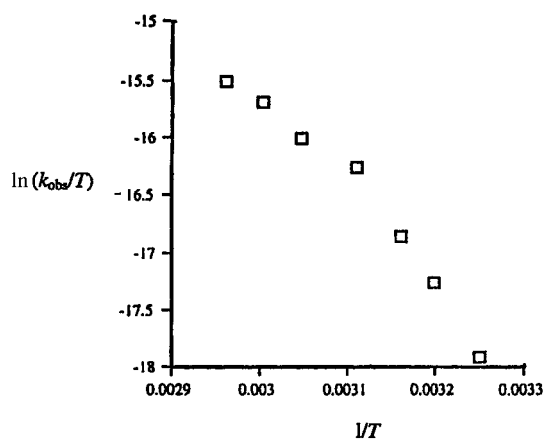


Figure 1. A plot of  $\ln(k_{\text{obs}}/T)$  vs.  $1/T$  for the reaction given in Equation (4).

the Eyring Equation (as predicted for Transition State Theory) and this is not surprising because we are not measuring the rate of a fundamental reaction step.<sup>[16]</sup> Even in the simplified reaction pathway shown in Scheme 1,  $k_3$ ,  $K_1$ , and  $K_2$  are all temperature dependent.

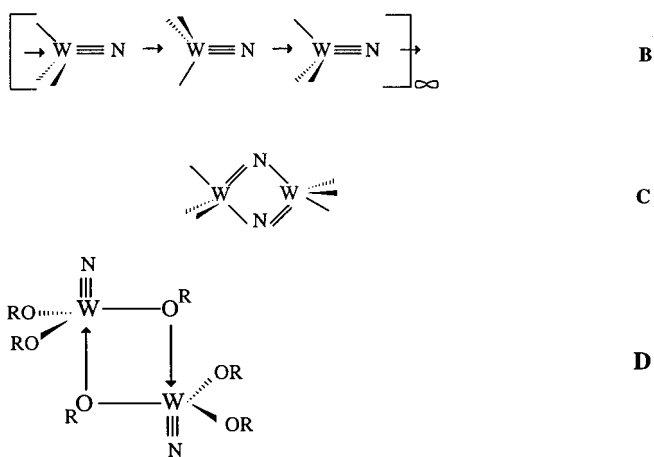
The complexity of the system does not allow us to speculate on the observed rate order of the cleavage of  $p\text{-X-C}_6\text{H}_4\text{CN}$ , where  $\text{X} = \text{CF}_3 > \text{Cl} > \text{H} > \text{OMe}$ , beyond noting that electronic factors will influence  $k_3$ ,  $K_1$ , and  $K_2$ . The total lack of reactivity of  $[\text{Mo}_2(\text{OCMe}_2\text{CF}_3)_6]$  over extended periods of time (weeks and months) is very striking, and we attribute this principally to factors influencing  $k_3$ . As we suggested in the

first paper in this series, the orbital energetics of the  $\pi$  and  $\pi^*$  orbitals of the substrate and M $\equiv$ M bond play an important role in controlling  $\Delta H^\ddagger$  for reductive cleavage.<sup>[4]</sup>

The reaction between  $[\text{W}_2(\text{OSiMe}_2t\text{Bu})_6]$  and PhCN was also studied. This too showed an equilibrium akin to that in Equation (2) and with time cleavage of the nitrile was observed to give  $[(t\text{BuMe}_2\text{SiO})_3\text{W}\equiv\text{N}]$  and PhC $\equiv$ CPh. No studies of the kinetics of this reaction were undertaken, but the similarity between  $[\text{W}_2(\text{OSiMe}_2t\text{Bu})_6]$  and  $[\text{W}_2(\text{OCMe}_2\text{CF}_3)_6]$  is noteworthy as in their reactions with CO.<sup>[17]</sup> In both cases these reactions differ notably when compared with  $[\text{W}_2(\text{OtBu})_6]$ .

### Molecular structures and spectroscopic studies of $(\text{RO})_3\text{W}\equiv\text{N}$ ,

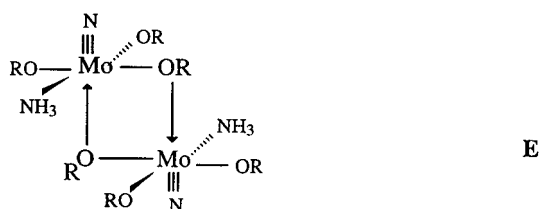
where  $\text{R} = t\text{BuMe}_2\text{Si}$  and  $\text{CF}_3\text{Me}_2\text{C}$ : The molecular structure of  $[(t\text{BuO})_3\text{WN}]$  is known to be that of a linear polymer with alternating long and short W–N distances that are typical of weak dative bonds and strong W–N triple bonds,<sup>[19]</sup> while the structure of  $[(\text{Ar}'\text{O})_3\text{WN}]$  was recently shown to be dimeric with a planar central  $\text{W}_2\text{N}_2$  moiety with alternating W–N distances.<sup>[20]</sup> Schematically these are shown in **B** and **C** below ( $\text{Ar}' = 2,6\text{-}i\text{Pr}_2\text{C}_6\text{H}_3$ ). It is therefore particularly interesting that the two compounds reported here represent two new structural types. For  $\text{R} = t\text{BuMe}_2\text{Si}$ , a combination of cryoscopic and spectroscopic data reveal that the compound is dimeric in solution with a structure of the type shown in **D**.



The cryoscopic molecular-weight determination in benzene gave  $M_w = 1052 \text{ g mol}^{-1}$  and in the  $^1\text{H}$  NMR there are two  $t\text{Bu}$  resonances in the integral ratio of 2:1 while the  $\text{SiMe}$  resonances appear as three singlets of equal intensity. The latter are consistent with the fact that at each W atom two of the RO ligands do not lie on a molecular plane of symmetry and so the  $t\text{BuMe}_2\text{Si}$  methyl groups of these ligands are diastereotopic. In the  $^{15}\text{N}$  NMR spectrum there is a single  $^{15}\text{N}$  signal for the labeled compound  $[(t\text{BuMe}_2\text{SiO})_3\text{W}^{15}\text{N}]_2$  flanked by tungsten satellites,  $J_{^{183}\text{W}-^{15}\text{N}} = 103 \text{ Hz}$  of integral intensity 14%, consistent with an  $^{15}\text{N}$  nucleus being bonded to a single W atom ( $^{183}\text{W}$ ,  $I = 1/2$ , 14.3% nat. abund.). Also in the infrared spectrum  $(\text{W}\equiv^{14}\text{N}) = 1169 \text{ cm}^{-1}$  and  $(\text{W}\equiv^{15}\text{N}) = 1138 \text{ cm}^{-1}$ , which support a terminal mode of bonding and can be compared with  $(\text{W}\equiv^{14}\text{N}) = 1014 \text{ cm}^{-1}$  ( $^{14}\text{N}$ ) and  $993 \text{ cm}^{-1}$  ( $^{15}\text{N}$ ) for  $[(t\text{BuO})_3\text{W}\equiv\text{N}]_\infty$ . Similarly in the trimeric

$[\text{Cp}^*\text{Ta}(\text{Me})\text{N}]_3$  ( $\text{Ta}-\text{N} = 960 \text{ cm}^{-1} (^{14}\text{N})$  and  $930 \text{ cm}^{-1} (^{15}\text{N})$ ) were reported.<sup>[3]</sup> [Unfortunately in the compound where  $\text{R} = \text{CF}_3\text{Me}_2\text{C}$  described in this work the value of ( $\text{W}\equiv\text{N}$ ) could not be assigned because of other resonances falling in this region.]

Although we do not have an X-ray structure of  $[(t\text{BuMe}_2\text{SiO})_3\text{WN}]_2$ , we finally should note that the proposed structure **D** is related to that seen for  $[\text{Mo}(\text{NO})(\text{O}i\text{Pr})_3]_2$ <sup>[21]</sup> and the ammonia adduct  $[\text{Mo}(\text{OSiMe}_3)_3(\text{N})(\text{NH}_3)]_2$ , which has the structure shown in **E**.<sup>[22]</sup> The solid-state molecular structure of



$[(\text{Me}_2\text{CF}_3\text{CO})_3\text{WN}]_3$  is shown in Figure 2. Selected bond distances and bond angles are given in Table 3. The coordination at each tungsten may be described in terms of a

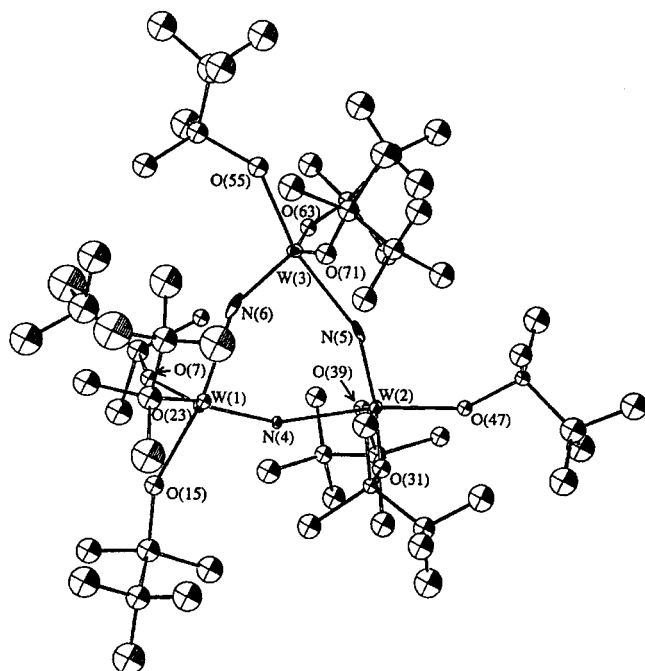


Figure 2. An ORTEP drawing of the cyclotrimer  $[(\text{Me}_2\text{CF}_3\text{CO})_3\text{WN}]_3$  giving the atom number scheme.

Table 3. Selected bond lengths [ $\text{\AA}$ ] and angles [ $^\circ$ ] for  $[\text{N}(\text{W}\equiv\text{OCMe}_2\text{CF}_3)_3]_3$ .

$\text{W}(1)-\text{N}(4)$	1.732(15)	$\text{W}(2)-\text{N}(5)$	1.682(19)
$\text{W}(3)-\text{N}(6)$	1.717(19)	$\text{W}(1)-\text{N}(6)$	2.159(20)
$\text{W}(3)-\text{N}(4)$	2.125(15)	$\text{W}(3)-\text{N}(5)$	2.159(18)
$\text{W}-\text{O}_{\text{ax}}$	1.904–1.913	$\text{W}-\text{O}_{\text{eq}}$	1.860–1.909
$\text{N}(4)-\text{W}(1)-\text{N}(6)$	84.9(7)	$\text{N}(4)-\text{W}(2)-\text{N}(5)$	84.9(7)
$\text{N}(5)-\text{W}(3)-\text{N}(6)$	87.6(7)	$\text{W}(1)-\text{N}(4)-\text{W}(2)$	154.5(10)
$\text{W}(2)-\text{N}(5)-\text{W}(3)$	153.6(9)	$\text{W}(1)-\text{N}(6)-\text{W}(3)$	150.7(9)
$\text{O}_{\text{ax}}-\text{W}-\text{N}_{\text{ax}}$	168(3) av	$\text{O}_{\text{ax}}-\text{W}-\text{N}_{\text{eq}}$	106(2) av
$\text{O}_{\text{ax}}-\text{W}-\text{O}_{\text{eq}}$	91(1) av	$\text{O}_{\text{eq}}-\text{W}-\text{O}_{\text{eq}}$	142(6) av
$\text{O}_{\text{eq}}-\text{W}-\text{N}_{\text{eq}}$	108(3) av		

distorted trigonal bipyramid, wherein two terminal RO ligands and the short  $\text{W}-\text{N}$  bond occupy equatorial sites and one terminal RO ligand and a long  $\text{W}-\text{N}$  bond are axial.

The solution NMR data ( $^1\text{H}$  and  $^{19}\text{F}$ ) support the existence of the trimeric structure in solution. There are two sets of RO ligands: three lie in the  $\text{W}_3\text{N}_3$  mirror plane, while six do not but are themselves related by the molecular mirror plane and the  $\text{C}_3$  axis of symmetry. The latter have diastereotopic Me groups. The  $^{15}\text{N}$  NMR spectra of the  $^{15}\text{N}$  labeled nitride complex show a singlet flanked by two sets of satellites due to coupling to  $^{183}\text{W}$ :  $J_{^{183}\text{W}-^{15}\text{N}} = 40$  and  $84$  Hz. Both sets of satellites have equal integral intensity  $\sim 14\%$ . Even upon heating to  $100^\circ\text{C}$  in  $[\text{D}_8]$ toluene the  $^{15}\text{N}$  spectrum remains unchanged indicating that the trimer does not dissociate and also that there is a significant barrier to the attainment of a symmetrically bridged cyclotrimer. Full data are given in the Experimental Section.

**Theoretical calculations:** Before examining the results of the geometry optimizations, some structural aspects of the  $\text{W}-\text{N}$  trimer structure deserve some comments. Each tungsten atom is five-coordinate in a local trigonal bipyramidal coordination and is bound to three alkoxide units, one of which is in an axial and two in equatorial positions. To complete the coordination spheres, the two nitrogen atoms occupy equatorial and axial sites. Formally, a double bond exists between the tungsten and equatorial nitrogen atoms and a single bond between  $\text{W}$  and the axial nitrogen. As expected for the trigonal bipyramidal environment, bonds from the metal to the equatorial sites are shorter than those to the axial sites.

Within the geometric constraints of the six-membered ring, it would also have been possible to have both nitrogens placed in equatorial positions, whereas the one equatorial nitrogen/one axial nitrogen conformation is observed. We have suggested<sup>[5]</sup> that whether or not both nitrogen atoms are in equatorial positions or one in an equatorial and the other axial orientation, an alternation of the  $\text{W}-\text{N}$  bond lengths around the ring is to be expected. The orbitals of the T-shaped  $\text{ML}_3$  fragment, even if symmetrically positioned with respect to the plane bisecting the  $\text{N}-\text{M}-\text{N}$  angle (both N in equatorial site), can induce a second-order Jahn–Teller distortion of the  $\pi$ -electron system that favors  $\text{M}-\text{N}$  bond alternation. Alternatively, a *fac*  $\text{ML}_3$  fragment bonds to equatorial and axial nitrogen atoms making the two centers intrinsically different. The preference for the *fac*  $\text{ML}_3$  arrangement is due to the large *trans* influence of the OR groups, which prefer to avoid a *mer* geometry where the two would be mutually *trans* to each other. Note that such an argument is based on the local requirements of the metal centers rather than the suggestion by Hoffmann and co-workers<sup>[1]</sup> and Wolczanski et al.<sup>[3]</sup> that the delocalization of electrons around the six-membered ring appears to favor equal  $\text{M}-\text{N}$  bond lengths in these types of systems. DFT calculations show that  $[\text{W}_3\text{N}_3\text{Cl}_6]$  is formed from three weakly interacting  $\text{WCl}_3\text{N}$  units and has a structure similar to  $[\text{W}_3\text{N}_3(\text{OR}_3)_6]$  with unequal  $\text{W}-\text{N}$  bonds.<sup>[23]</sup>

With these arguments in mind, it is easy to understand why equivalent  $\text{Ta}-\text{N}$  bond distances are observed for the first two metal-nitride trimers prepared. Each tantalum center is located in a pseudotetrahedral environment, if the cyclo-

pentadienyl (Cp) rings are considered to occupy one coordination site about the metal. The plane going through the center of Cp, which also contains Ta and X, bisects the N–Ta–N angle. The local coordination around Ta makes the two Ta–N bonds potentially equivalent. The five-coordinate environment around each metal center, as it occurs in the tungsten-nitride trimer, is central to the nonequivalence of the W–N bonds and thus the only situation with alternating bond lengths around the ring.

In support of this analysis, an extended Hückel calculation of the W–N trimer with all equal W–N bond lengths and the experimental position for the OR group (modeled by OH) gives a larger W–N Mulliken overlap population for the equatorial nitrogen; this is an indication for a shorter bond length.<sup>[5]</sup> This qualitative analysis needs to be complemented by a more quantitative theoretical study. DFT(B3LYP) calculations have been used with the purpose to attempt a better understanding of the bond alternation in the W–N ring, the relation between the W–N distances, and the site occupancy of the alkoxy group as well as to propose some interpretation of the slow exchange between W–N short and long bond lengths.

The structure of  $[(\text{HO})_3\text{WN}]_3$  was optimized with no symmetry constraint (Figure 3). The three W and the three N centers form a planar six-membered ring with alternating

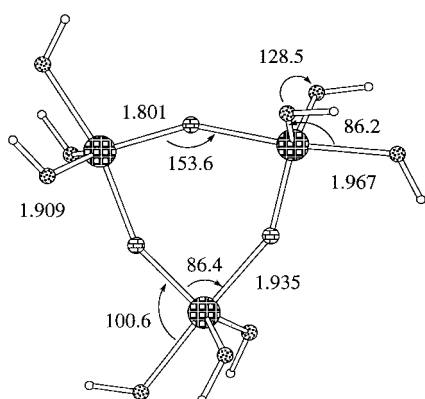


Figure 3. Optimized DFT (B3LYP) structure for  $[(\text{HO})_3\text{WN}]_3$ . Selected bond lengths in Å and angles in degrees.

short (1.801) and long (1.935 Å) W–N distances and  $C_3$  symmetry. The three OH groups complete the coordination of the metal to form a local trigonal bipyramid. The axial OH group ( $\text{W–O} = 1.967$  Å) of the bipyramid is opposite to the long W–N bond ( $\text{N–W–O} = 172.8^\circ$ ). The two other OH groups with shorter W–O distances (1.909 Å) occupy the equatorial site ( $\text{O}_{\text{ax}}\text{–W–O}_{\text{eq}} = 115.5^\circ$ ). The N–W–N and W–N–W angles are  $86.4$  and  $153.6^\circ$ , respectively. Note, changing the orientation of the equatorial OH groups (to point toward N and not toward axial OH) gave qualitatively similar results. These structural features are in good qualitative agreement with the experimental data and highlight the preference for the alternating short–long distances and the planar  $(\text{W–N})_3$  six-membered ring. They also show that the three OH groups have a preference to occupy one axial and two equatorial sites of the trigonal bipyramid and not two

axial and one equatorial. Hence, the OH groups prefer not to lie in the same plane and could be defined, for convenience, as being *fac* as opposed to *mer* (corresponding to two axial and one equatorial site). This shows that the preference for *fac* over *mer*, not imposed by the steric hindrance of the OR groups, forces the nitrogen atoms to occupy two nonequivalent sites, that is, equatorial and axial sites of the local trigonal bipyramid. The alternation of short and long W–N bonds comes from a local property of each metal center and not as a result of a collective effect in the six-membered ring. The optimized structure of the monomer  $\text{WN}(\text{OH})_3$  ( $\text{W–N} = 1.670$  Å,  $\text{W–O} = 1.9121$  Å,  $\text{O–W–N} = 103.3^\circ$ ) is very similar to that calculated for  $\text{WNCl}_3$ .<sup>[23]</sup> The bonding interaction in the trinuclear system is calculated to be  $25.6$  kcal mol<sup>−1</sup> per monomer, which is also similar to that in  $\text{W}_3\text{N}_3\text{Cl}_9$  despite the fact that the WN bond is significantly more stretched in the trimer for the alkoxy groups than for chloride ligands.

A complete search for a transition state (TS) for exchanging the equatorial and axial OH and thus simultaneously interconverting the short and long W–N bonds is impractical owing to the large size of the system. An estimate of the mechanism to exchange short and long W–N bonds was carried out in the following way. Since the two nitrogen atoms are part of a ring, the pseudorotation at W would preferably occur through a turn-style mechanism and not a Berry rotation. The three  $\text{W}(\text{OR})_3$  moieties can rotate in the same direction (clockwise for instance) or one in the opposite direction of the two other groups. If the first case, the TS would have a  $C_{3v}$  symmetry and in the second case it would have a  $C_s$  symmetry going through the unique metal that rotates in a different manner from the two other. The optimization of the two model TSs under these symmetry constraints have been carried out. A search with a *mer* arrangement of the OH groups proved to be unsuccessful, since it falls back to the minimum structure.

The  $C_s$  structure (Figure 4) is  $16$  kcal mol<sup>−1</sup> above the optimized minimum, while the  $C_{3v}$  species (Figure 5) is even higher ( $23$  kcal mol<sup>−1</sup>). These high energies, in species already deprived from steric factors, rationalize the lack of fluxionality in the real system.

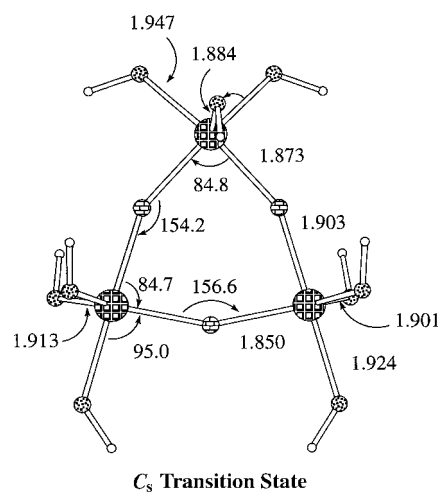


Figure 4. Optimized geometry of a model of the  $C_s$  transition state for interchanging short and long W–N bonds.

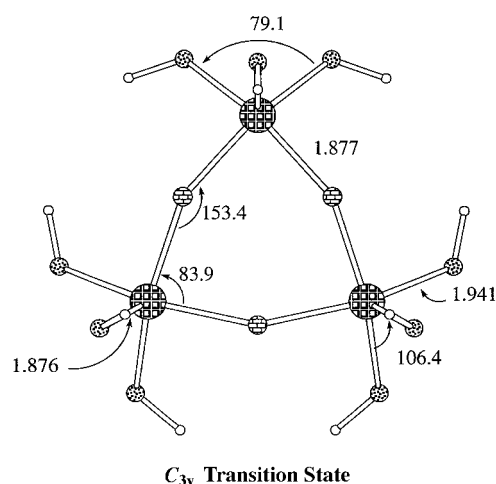


Figure 5. Optimized geometry of a model of the  $C_{3v}$  transition state for interchanging short and long W–N bonds.

The  $C_s$  geometry allows two equivalent W–N distances (1.873 Å) around one metal center only. The two other metal centers have short and long W–N distances. The coordination sphere around the unique W atom with equal W–N distances is a square-based pyramid, while the trigonal bipyramidal arrangement is found for the two other metals. The  $C_{3v}$  geometry has all equal W–N distances (1.877 Å). Each metal center has a square-pyramidal geometry. The six-membered ring remains essentially planar.

It should be pointed out that for the  $C_s$  or the  $C_{3v}$  transition states, there are no major changes in the geometry of the ring in terms of angles at the N or at the W centers. The W–N distances are also not drastically different from the one found in the minimum.

The analytical frequencies were calculated with Gaussian 98 (see Computational Details). The  $C_s$  type transition state has one very negative eigenvalue ( $-222\text{ cm}^{-1}$ ) and another smaller one ( $-99\text{ cm}^{-1}$ ). Examination of the vibration associated with the more negative value shows a significant participation of the antisymmetric W–N stretch frequency mixed with a displacement of the apical OH group at the unique square-based pyramidal W center. The less negative eigenvalue corresponds only to motion of the OH groups. In the  $C_{3v}$  type transition state, there are four negative frequencies. The most negative one ( $-285\text{ cm}^{-1}$ ) involves the stretch of the W–N bonds together with the motion of the apical OH as in the  $C_s$  type TS. The three other less negative frequencies ( $-88$ ,  $-68$ , and  $-66\text{ cm}^{-1}$ ) involve mostly motion of the OH groups. Thus, the  $C_s$  type TS seems to be a better model of the true TS than the  $C_{3v}$  type TS. This indicates that the equivalency of the W–N bonds should be obtained through a turnstile pseudorotation mechanism in which each W center goes sequentially from a trigonal bipyramidal coordination to a square pyramidal coordination.

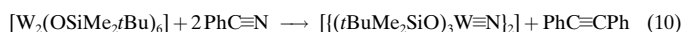
In conclusion, the preference for alternate short/long W–N distances is very pronounced and is probably associated with the preference for a trigonal bipyramidal coordination of the metal center; this forces the two N centers to occupy two nonequivalent sites (equatorial and axial) of the trigonal

bipyramid. While the transition state for N site exchange could not be fully located, our models for the transition states provide some insight into the process. The site-exchange process probably involves the sequential pseudorotation at one tungsten at a time to form a local square-based pyramid. In contrast to what is known in pentacoordination, the energy associated with this site-exchange process is unusually high and does not seem to be lowered by any collective process associated with the ring.

## Conclusion

The present work provides two new structural types for  $d^0$  metal nitrides of empirical formula  $(\text{RO})_3\text{WN}$ : a dimer with terminal nitrides and bridging RO ligands when  $\text{R} = t\text{BuMe}_2\text{Si}$  and a cyclootrimer when  $\text{R} = \text{Me}_2\text{CF}_3\text{C}$ . The latter has a planar  $\text{W}_3\text{N}_3$  ring with alternating short and long distances. These structures are evidently present in the solid state and solution and contrast with the previous linear polymeric nitride chain for  $\text{R} = t\text{Bu}$  and the nitride-bridged dimer for  $\text{Ar}' = 2,5\text{-}i\text{Pr}_2\text{-C}_6\text{H}_3$ . The rationale for the nondelocalized cyclootrimer arises from the attendant  $(\text{RO})_3\text{M}$  fragment in contrast to the  $\text{Cp}(\text{X})\text{M}$  fragment found for the tantalum complexes by Roesky<sup>[2]</sup> and Wolczanski.<sup>[3]</sup>

At this point it is worth considering the cleavage of dinitrogen in the hypothetical reaction shown in Equation (9) as compared with that observed for benzonitrile in Equation (10). If we consider Equation (10) in terms of only the bonds formed and broken, we can write the expression given in Equation (11).



$$\Delta H^\circ [\text{Eq. (10)}] = -2[\Delta H^\circ(\text{W}\equiv\text{N})] - \Delta H^\circ(\text{C}\equiv\text{C}) + \Delta H^\circ(\text{W}\equiv\text{W}) + 2[\Delta H^\circ(\text{C}\equiv\text{N})] \quad (11)$$

Taking average values for  $\Delta H^\circ$  for C–C and C–N triple bonds<sup>[24]</sup> as  $-194\text{ kcal mol}^{-1}$  and  $-213\text{ kcal mol}^{-1}$ , respectively, and assuming that the reaction is thermoneutral, that is,  $\Delta H^\circ [\text{Eq. (10)}] = 0$  (although we know it is thermodynamically favored and thus  $\Delta H [\text{Eq. (10)}]$  is negative) we can write:  $-2[\Delta H^\circ(\text{W}\equiv\text{N})] + \Delta H^\circ(\text{W}\equiv\text{W}) = -232\text{ kcal mol}^{-1}$ . Thus, knowing  $\Delta H^\circ(\text{N}\equiv\text{N}) = 226\text{ kcal mol}^{-1}$ ,<sup>[25]</sup> we can estimate that the reductive cleavage of dinitrogen as expressed by Equation (9) is thermodynamically favorable by more than  $6\text{ kcal mol}^{-1}$ . Certainly we can conclude that reductive cleavage does not occur because of kinetic rather than thermodynamic factors. It is also interesting to note that if we take the value of  $\Delta H^\circ(\text{W}\equiv\text{W})$  to be  $80\text{ kcal mol}^{-1}$ , as is indicated by calculations,<sup>[26]</sup> then  $\Delta H^\circ(\text{W}\equiv\text{N})$  is  $156\text{ kcal mol}^{-1}$ . If the value of  $\Delta H^\circ(\text{W}\equiv\text{W})$  has as an upper limit value of  $100\text{ kcal mol}^{-1}$ , then  $\Delta H^\circ(\text{W}\equiv\text{N})$  would still be greater than  $136\text{ kcal mol}^{-1}$ , which is in good agreement with expectations based on an analogy with  $\Delta H^\circ(\text{W}\equiv\text{O})$  bond strengths for  $d^0$  tungsten complexes.<sup>[27]</sup> These suggestions concerning the thermodynamic favorability of Equation (9) are consistent with the

recent findings by Cummins et al.<sup>[28]</sup> who have showed that various  $X_3Mo$  complexes will cleave  $N\equiv N$  and that this reaction may be coupled with  $[(tBuO)_3Mo\equiv N]$  and  $[Mo_2(O-tBu)_6]$ .

In conclusion, we believe that this work brings us further in our understanding of the cleavage of C–X multiple bonds in their reactions with M–M triple bonds, but clearly there are a number of matters that still warrant further attention, and future studies are planned to elucidate further upon electronic factors associated with the reductive cleavage reaction.

## Experimental Section

All operations were carried out under a dry and oxygen free atmosphere of  $N_2$ , with the use of dry and oxygen free solvents with standard Schlenk, vacuum-line, and dry-box handling procedures. The compounds  $[M_2(OR)_6]$ , where  $M=Mo$  and  $W$ , were prepared from  $[M_2(NMe_2)_6]$  by alcoholysis ( $R=tBuMe_2Si$  and  $CF_3Me_2C$ ).<sup>[29]</sup> The nitriles (from Aldrich) were distilled and subjected to three freeze–thaw degas cycles and stored over 4 Å molecular sieves prior to use. The NMR spectra were recorded on a Bruker AM500 spectrometer in  $[D_8]toluene$  as solvent.  $^{15}N$  chemical shifts are in ppm relative to the external reference of neat  $MeC\equiv^{15}N$  set at  $\delta$  135.3.  $^{13}C$  and  $^1H$  chemical shifts are referenced to the  $^{13}C$  and proton impurity signals in  $[D_8]toluene$ .  $^{19}F$  NMR signals are referenced to external  $CF_3COOH$ . The dynamic behavior of the equilibrium between  $[M_2(OR)_6]$  complexes with  $MeC\equiv^{15}N$  was studied by  $^{15}N$  NMR spectroscopy with the line-shape analysis program DNMR5.<sup>[30]</sup> The nitrile cleavage reaction involving  $Ph^{13}C\equiv N$  was monitored by  $^{13}C\{^1H\}$  NMR spectroscopy. The  $T_1$  relaxation times for benzonitrile (14.5 s) and diphenylacetylene (11.4 s)  $^{13}C$  signals were measured at 48.6 °C. The Ernst equation, Equation (12) [where  $t_1 = T_1$  relaxation time,  $pw = 90^\circ$  pulse width,  $at =$  acquisition time, and  $d_1 =$  delay time between pulses], was used to determine the optimal pulse widths for the delay time used in NMR experiments.<sup>[31]</sup>

$$pw = \cos^{-1}(\exp^{-(at+d_1)t_1})(pw \ 90/360) \quad (12)$$

Thermodynamic and kinetic measurements were performed with temperatures calibrated with a sample of neat methanol and van Greet's equation.<sup>[31a]</sup> The volumes of the samples, which were prepared at  $-23^\circ C$ , were adjusted to the temperature at which the NMR experiments were performed. This was accomplished by use of the cubical expansion of toluene and benzene.<sup>[32]</sup>

**Preparation of isotopically labeled nitriles:** The appropriate  $^{13}C$  or  $^{15}N$  labeled nitrile was synthesized by a slightly modified version of a literature procedure.<sup>[33]</sup> KCN (1.03 g, 15.1 mmol) and  $[Pd(PPh_3)_4]$  (150 mg, 0.13 mmol) were added to a 30 mL Schlenk flask. Dimethoxyethane (DME; 5 mL) was added by cannula. In a separate 30 mL Schlenk flask PhI (2.45 g, 12.1 mmol) was dissolved in DME (5 mL). The PhI solution was combined with the KCN/DME solution. The flask was equipped with a reflux condenser, and the mixture was heated to boiling for 24 h. The solution was filtered to remove solids followed by fractional distillation to purify and collect the  $PhC\equiv N$  (b.p. 188 °C, 760 Torr).

**Preparation of samples for the determination of kinetics:** The samples were prepared in a He filled glove box. For the runs where the temperature was varied,  $[W_2(OCMe_2CF_3)_6]$  (10.0 mg,  $8.85 \times 10^{-3}$  mmol) was added to an NMR tube equipped with a J. Young<sup>®</sup> adapter. The  $^{13}C$  labeled benzonitrile (500  $\mu L$  of a stock solution) was added through a gas-tight syringe. The stock solution was prepared by adding  $Ph^{13}C\equiv N$  (462.5 mg,  $4.42 \times 10^{-3}$  mmol) to a 25 mL volumetric solution flask followed by addition of  $[D_6]benzene$  to the mark on the volumetric flask. The stock solution was transferred to a flask equipped with a Kontes<sup>®</sup> valve and stored over 4 Å sieves. For the reactions at 48.6 °C where the concentration of benzonitrile was varied, the appropriate volume of stock solution was delivered through a gas-tight syringe (150  $\mu L$  for three equivalent experiments) to bring the total volume in the NMR tube to 500  $\mu L$ . To prepare the sample with two equivalents of benzonitrile, the same general method was followed with

100  $\mu L$  of stock solution added to an NMR tube charged with the tungsten complex, followed by the addition of 400  $\mu L$  of  $[D_6]benzene$ . In all reactions the rate of formation of  $Ph^{13}C\equiv^{13}CPh$ ,  $\delta^{13}C = 90.2$ , was followed.

**Preparation of  $[(CF_3Me_2CO)_3WN]_3$ :** Benzonitrile (150  $\mu L$ , 1.5 mmol) was added to a solution of  $[W_2(OCMe_2CF_3)_6]$  (170 mg, 0.15 mmol) in dry, degassed benzene (10 mL) at 25 °C. The solution was stirred for 24 h at 25 °C, and the solvent was then removed under vacuum. Recrystallization from hexanes gave X-ray quality pale orange crystals in 68% yield upon cooling to  $-20^\circ C$ .  $^1H$  NMR at 24 °C:  $\delta = 1.52$  (6H), 1.54 (6H), 1.60 (6H);  $^{15}N$  NMR:  $\delta = 216.6$ ,  $J_{^{15}N-W} = 84$  Hz (14%), 40 Hz (14%);  $^{19}F$  NMR  $\delta = -84.2$  (6F),  $-83.6$  (12F).

**Preparation of  $[(tBuMe_2SiO)_3WN]_2$ :** Benzonitrile (150  $\mu L$ , 1.5 mmol) was added to a solution of  $[W_2(OSiMe_2tBu)_6]$  (173 mg, 0.15 mmol) in benzene (10 mL) at 25 °C. The solution was stirred for 24 h at 25 °C and the solvent was reduced to 2 mL under a dynamic vacuum. Dry, degassed MeCN (10 mL) was added, and the solution was filtered. The solids were washed with acetonitrile (2 mL), dried, and collected to yield the title compound as a tan powder (78% yield).  $^1H$  NMR, 24 °C:  $\delta = 0.25$  (12H), 0.31 (12H), 0.32 (12H), 1.09 (18H), 1.12 (36H);  $^{15}N$  NMR:  $\delta = 6.5$ ,  $J_{^{15}N-W} = 103$  Hz (14%); IR (nujol)  $\tilde{\nu} = 1169$  ( $W\equiv^{14}N$ ), 1138  $cm^{-1}$  ( $W\equiv^{15}N$ ); for  $[(tBuO)_3W\equiv N]_{\infty}$   $\tilde{\nu} = 1014$  ( $W\equiv^{14}N$ ), 993  $cm^{-1}$  ( $W\equiv^{15}N$ ).

**$[M_2(OR)_6(N)(CR')_2]$ :** Selected NMR data in  $CD_2Cl_2$ :  $[W_2(OCMe_2CF_3)_6(^{15}NCMe)_2]$   $^{15}N$  NMR:  $\delta = 170.0$ ;  $[Mo_2(OCMe_2CF_3)_6(^{15}NCMe)_2]$   $^{15}N$  NMR ( $-40^\circ C$ ):  $\delta = 100.1$ ;  $[W_2(OCMe_2CF_3)_6(N^{13}CPh)_2]$  ( $-30^\circ C$ )  $^{13}C\equiv N$ :  $\delta = 136.4$ ;  $^1H$  NMR for  $CMe_2CF_3$ :  $\delta = 2.18, 1.14, 1.02$  (singlets of equal intensity).

**Crystal and molecular structure of  $[(Me_2CF_3CO)_3WN]_2$ :** A listing of programs and operating procedures has been previously given.<sup>[34]</sup> A summary of crystal data is given in Table 4. Further details of the crystal

Table 4. Summary of crystal data for  $[WN(OCMe_2CF_3)_3]_3$ .

$M_w$	1744.4
space group	$P2_1/c$
$T$ [°C]	$-170$
$a$ [Å]	22.481(5)
$b$ [Å]	11.367(2)
$c$ [Å]	22.573(4)
$\beta$ [°]	94.60(1)
$V$ [Å <sup>3</sup> ]	5749.7
$Z$	4
$\rho_{calcd}$ [g cm <sup>-3</sup> ]	2.015
$\lambda$ [Å]	0.71069
linear absorption coefficient	62
$R(F)^{[a]}$	0.0503
$R_w(F)^{[b]}$	0.0513

[a]  $R(F) = \sum |F_o| - |F_c| / \sum |F_o|$ . [b]  $R_w(F) = \{w(|F_o| - |F_c|)^2 / w|F_o|^2\}^{1/2}$ , where  $w = 1/[\sigma^2 |F_o|]$ .

structure investigation can be obtained from the Fachinformationszentrum Karlsruhe, D-76344 Eggenstein-Leopoldshafen (Germany) (fax: (+49) 7247-808-666; e-mail: crysdata@fiz.karlsruhe.de) on quoting the depositary number CDS-58362. Full details are available through the reciprocal database at <http://www.iurnsc.indiana.edu/>. Request report no. 94018.

**Computational details:** Preliminary calculations proved that RHF level was not sufficient. Poor results were also obtained with calculations including 68 electrons in the effective core potential of W. Thus all calculations were carried out with the Gaussian 94 package of programs<sup>[35]</sup> at the B3LYP computational level.<sup>[36]</sup> Effective core potentials were used for replacing the 60 innermost electrons of W.<sup>[37]</sup> The basis set was of valence double- $\zeta$  quality with polarization functions on N and O.<sup>[38]</sup> All geometries presented were characterized as zero-gradient stationary points through the analytical computation of gradients. Owing to the large size of the systems, symmetry restrictions were introduced where mentioned. During the revision stage process Gaussian 98 was made available.<sup>[39]</sup> This program was used to calculate the analytical frequencies of the  $C_s$  and  $C_{3v}$  types transition states.



## Acknowledgment

The authors thank the National Science Foundation and the CNRS (PICS) for an International US/France Grant. Also we thank Professor T. A. Budzichowski for both technical assistance in the measurement of thermodynamic and kinetic parameters and stimulating discussions.

- [1] R. A. Wheeler, R. Hoffman, J. Strähle, *J. Am. Chem. Soc.* **1986**, *108*, 5381.
- [2] H. Plenio, H. W. Roesky, M. Noltemeyer, G. M. Sheldrick, *Angew. Chem.* **1988**, *100*, 1337; *Angew. Chem. Int. Ed. Engl.* **1988**, *27*, 1330.
- [3] M. M. Bernaszk-Holl, M. Kersting, B. D. Pendley, P. T. Wolczanski, *Inorg. Chem.* **1990**, *29*, 1518.
- [4] For a study of the cleavage of C=S bonds see T. A. Budzichowski, M. H. Chisholm, K. Foltling, *Chem. Eur. J.* **1996**, *2*, 110.
- [5] M. H. Chisholm, K. Foltling, D. B. Tiedtke, F. Lemoigno, O. Eisenstein, *Angew. Chem.* **1995**, *107*, 61; *Angew. Chem. Int. Ed. Engl.* **1995**, *34*, 110.
- [6] For PES data on a series of  $[M_2(NMe_2)_2(OR)_4]$  compounds see M. H. Chisholm, N. Gruhn, D. Lichtenberger, D. B. Tiedtke, *Polyhedron* **1998**, *17*, 705.
- [7] R. R. Schrock, M. L. Listemann, L. G. Sturgeoff, *J. Am. Chem. Soc.* **1982**, *104*, 4291.
- [8] J. H. Freudenberger, S. F. Pedersen, R. R. Schrock, *Bull. Soc. Chim. France* **1985**, 349.
- [9] F. A. Cotton, G. Wilkinson, in *Advanced Inorganic Chemistry*, 5th ed., Wiley, **1988**.
- [10] For the formation of  $PhC\equiv CPh$  in the reaction between  $PhC(W\equiv OR)_3$  and  $PhC\equiv N$ , see M. L. Listemann, R. R. Schrock, *Organometallics* **1985**, *4*, 74, and references therein.
- [11] M. H. Chisholm, J. C. Huffman, N. S. Marchant, *J. Am. Chem. Soc.* **1983**, *105*, 6162.
- [12] J. L. Eglin, E. M. Hines, E. J. Valente, J. D. Zubkowski, *Inorg. Chem. Acta* **1995**, *229*, 113.
- [13] F. A. Cotton, F. E. Kuhn, *J. Am. Chem. Soc.* **1996**, *118*, 5826.
- [14] a) M. H. Chisholm, K. Foltling, D. M. Hoffman, J. C. Huffman, *J. Am. Chem. Soc.* **1984**, *106*, 6794; b) M. H. Chisholm, B. K. Conroy, J. C. Huffman, N. S. Marchant, *Angew. Chem.* **1986**, *98*, 448; *Angew. Chem. Int. Ed. Engl.* **1986**, *25*, 446; c) M. H. Chisholm, K. Foltling, J. C. Huffman, E. A. Lucas, *Organometallics* **1991**, *10*, 535.
- [15] P. T. Wolczanski, R. L. Miller, A. L. Rheingold, *J. Am. Chem. Soc.* **1993**, *115*, 10422.
- [16] See R. G. Wilkins, *Kinetics and Mechanisms of Reactions of Transition Metal Complexes*, 2nd ed., VCH, **1991**, p. 89, section 2.3.2.
- [17]  $[W_2(OR)_6(CO)_2]$  for  $R = SiMe_2tBu$  and  $Me_2CF_3C$ : T. A. Budzichowski, M. H. Chisholm, D. B. Tiedtke, J. C. Huffman, W. E. Streib, *Organometallics* **1995**, *14*, 2318.
- [18]  $[W_2(OtBu)_6(CO)]$ : M. H. Chisholm, D. M. Hoffman, J. C. Huffman, *Organometallics* **1985**, *4*, 986.
- [19] M. H. Chisholm, D. M. Hoffman, J. C. Huffman, *Inorg. Chem.* **1983**, *22*, 2903.
- [20] T. A. Pollagi, J. Manna, S. J. Geib, M. D. Hopkins, *Inorg. Chim. Acta* **1996**, *243*, 177.
- [21] M. H. Chisholm, F. A. Cotton, M. W. Extine, R. L. Kelly, *J. Am. Chem. Soc.* **1978**, *100*, 3354.
- [22] G. S. Kim, C. W. DeKock, *J. Chem. Soc. Chem. Commun.* **1988**, 1166.
- [23] W. W. Schoeller, A. Sundermann, *Inorg. Chem.* **1998**, *37*, 3034.
- [24] T. H. Lowry, K. S. Richardson, in *Mechanisms and Theory in Organic Chemistry*, 3rd ed., Harper Row, New York, **1987**.
- [25] H. B. Gray, R. L. DeKock, in *Chemical Structure and Bonding*, 2nd ed., University Science Books, Mill Valley, CA, **1989**.
- [26] F. A. Cotton, R. A. Wilkinson, in *Multiple Bonds Between Metal Atoms*, 2nd ed., Oxford University Press, **1996**.
- [27] For estimates of metal-oxo bond strengths see: R. H. Holm, *Polyhedron* **1993**, *12*, 571.
- [28] a) C. C. Cummins, C. E. Laplaza, *Science* **1995**, *268*, 861; b) C. E. Laplaza, A. L. Odom, W. M. Davis, C. C. Cummins, J. D. Protasiewicz, *J. Am. Chem. Soc.* **1995**, *117*, 4999; c) C. E. Laplaza, A. R. Johnson, C. C. Cummins, *J. Am. Chem. Soc.* **1996**, *118*, 709.
- [29]  $[Mo_2(OR)_6]$ :  $R = tBu$ , M. Akiyama, M. H. Chisholm, F. A. Cotton, M. W. Extine, D. A. Haitko, D. Little, P. E. Fanwick, *Inorg. Chem.* **1979**, *18*, 2266;  $R = Me_2tBuSi$ , M. H. Chisholm, C. M. Cook, J. C. Huffman, W. E. Streib, *J. Chem. Soc. Dalton Trans* **1991**, 929;  $R = Me_2CF_3C$ , ref. [8].
- [30] Program available upon request from QCPE, Indiana University, Bloomington, IN 47405.
- [31] a) *VNMR Command and Parameter Reference Manual*, VNMR Version 5.2 Software, Varian Associates, Palo Alto, CA, **1995**, p. 168; b) R. R. Ernst, W. A. Anderson, *Rev. Sci. Instr.* **1966**, *37*, 93.
- [32] D. W. Green, J. O. Maloney, in *Perry's Chemical Engineers' Handbook*, 6th ed., McGraw Hill, New York, **1984**.
- [33] A. Sekiya, N. Ishikawa, *Chem. Lett.* **1975**, 277.
- [34] M. H. Chisholm, K. Foltling, J. C. Huffman, C. C. Kirkpatrick, *Inorg. Chem.* **1984**, *23*, 1021.
- [35] M. J. Frisch, G. W. Trucks, H. B. Schlegel, P. M. Gill, B. G. Johnson, M. A. Robb, J. R. Cheeseman, T. Keith, G. A. Petersson, J. A. Montgomery, K. Raghavachari, M. A. Al-Laham, V. G. Zakrzewski, J. V. Ortiz, J. H. Foresman, C. Y. Peng, P. Y. Ayala, W. Chen, M. W. Wong, J. L. Andres, E. S. Replogle, R. Gomperts, R. L. Martin, D. J. Fox, J. S. Binkley, D. J. Defrees, J. Baker, J. P. Stewart, M. Head-Gordon, C. Gonzalez, J. A. Pople, *Gaussian 94*, Gaussian, Pittsburgh, PA **1995**.
- [36] A. D. Becke, *J. Chem. Phys.* **1993**, *98*, 5648; C. Lee, W. Yang, R. G. Parr, *Phys. Rev. B* **1988**, *37*, 785; P. J. Stephens, F. J. Devlin, C. F. Chabalowski, M. Frisch, *J. Phys. Chem.* **1994**, *98*, 11623.
- [37] P. J. Hay, W. R. Wadt, *J. Chem. Phys.* **1985**, *82*, 299.
- [38] T. H. Dunning, P. J. Hay, *Modern Theoretical Chemistry* (Ed.: H. F. Scafer, III), Plenum, New York, **1977**, pp. 1–28.
- [39] M. J. Frisch, G. W. Trucks, H. B. Schlegel, G. E. Scuseria, M. A. Robb, J. R. Cheeseman, V. G. Zakrzewski, J. A. Montgomery, Jr., R. E. Stratmann, J. C. Burant, S. Dapprich, J. M. Millam, A. D. Daniels, K. N. Kudin, M. C. Strain, O. Farkas, J. Tomasi, V. Barone, M. Cossi, R. Cammi, B. Mennucci, C. Pomelli, C. Adamo, S. Clifford, J. Ochterski, G. A. Petersson, P. Y. Ayala, Q. Cui, K. Morokuma, D. K. Malick, A. D. Rabuck, K. Raghavachari, J. B. Foresman, J. Cioslowski, J. V. Ortiz, B. B. Stefanov, G. Liu, A. Liashenko, P. Piskorz, I. Komaromi, R. Gomperts, R. L. Martin, D. J. Fox, T. Keith, M. A. Al-Laham, C. Y. Peng, A. Nanayakkara, C. Gonzalez, M. Challacombe, P. M. W. Gill, B. Johnson, W. Chen, M. W. Wong, J. L. Andres, C. Gonzalez, M. Head-Gordon, E. S. Replogle, J. A. Pople, *Gaussian 98, Revision A6*, Gaussian, Pittsburgh, PA, **1998**.

Received: February 6, 1998

Revised version: April 30, 1999 [F 986]